

Received: February 13, 2025; Accepted: June 10, 2025; Published: July 1, 2025.

DOI. 10.30473/coam.2025.73804.1289

Summer-Autumn (2025) Volume 10, Issue 2, (213-240)

Research Article

Open a

## Control and Optimization in Applied Mathematics - COAM

# **Hybrid RBF Method for Solving Fractional PDE-Constrained Optimal Control Problems**

Maha Mohsin Mohammed Ali $^{1,2} oxtimes^{m{0}}$ , Mahmoud Mahmoudi $^{1} ar{^{0}}$ , Majid Darehmiraki $^{3} ar{^{0}}$ 

<sup>1</sup> Department of Mathematics, College of Science, University of Qom, Qom, Iran.

<sup>2</sup>Department of Information and Communication Technology, Baghdad Institute of Technology, Middle Technical University, Baghdad, Iraq.

<sup>3</sup>Department of Mathematics, Behbahan Khatam Alanbia University of Technology, Khouzestan, Iran.

## $\boxtimes$ Correspondence:

Maha Mohsin Mohammed Ali **E-mail:** 

Maha.ali2015.ma@mtu.edu.iq **How to Cite** 

Maha Mohsin M.A., Mahmoudi, M., Darehmiraki, M. (2025). "Hybrid RBF method for solving fractional PDE-constrained optimal control problems", Control and Optimization in Applied Mathematics, 10(2): 213-240, doi: 10.30473/coam.2025.73804.1289.

**Abstract.** This study addresses the numerical solution of an optimal control problem governed by a fractional convection-reactiondiffusion partial differential equation. The approach utilizes Radial Basis Function-Partition of Unity (RBF-PU) methods combined with the Gr"unwald-Letnikov approximation for fractional derivatives, which provides a fundamental extension of classical derivatives in fractional calculus. To enhance sparsity in the control strategy, an  $L_2$ norm is integrated into the objective function, along with quadratic penalties to reduce deviations from the desired state. This hybrid formulation facilitates the effective management of spatially sparse controllers, relevant in many practical applications. The RBF-PU technique offers a flexible and efficient framework by partitioning the domain into overlapping subregions, applying local RBF approximations, and synthesizing the global solution with compactly supported weight functions. Numerical experiments demonstrate the accuracy and effectiveness of this method.

**Keywords.** Local RBF approximation, Heat equation, Fractional derivative, Optimal control,  $L_2$  norm.

MSC. 49M41; 82M22.

https://mathco.journals.pnu.ac.ir

#### 1 Introduction

In many applications, classical differential equations are insufficient to accurately model the complexity of physical processes; instead, partial differential equations (PDEs) are essential tools for capturing spatial and temporal variations across diverse systems. These PDEs are fundamental in formulating control problems (Optimal Control Issues, or OCI) across a broad range of scientific and engineering disciplines, acting as the backbone for modeling phenomena with spatial-temporal dependencies. They underpin the mathematical description of numerous physical phenomena, such as heat transfer, where temperature gradients evolve over time and space, dispersion processes involving chemicals spreading through media, electromagnetic wave propagation in three dimensions, fluid dynamics influenced by velocity, pressure, and external forces, as well as phase change processes like freeze-thaw cycles, which are critical in materials science, climate modeling, and environmental studies.

The robustness of PDE-based models enables more detailed and accurate analysis of these complex systems, improving the precision and effectiveness of control and optimization strategies, especially in real-world applications where system behavior is inherently multi-dimensional and dynamic. As a result, PDE-based optimal control problems are increasingly relevant, serving as foundational tools in designing efficient, sustainable, and innovative solutions across various fields. For instance, fractional models, where derivatives of non-integer order are used, have gained prominence for better capturing anomalous diffusion and memory effects present in complex systems [3, 30, 20].

Over recent decades, significant advancements have been made in the numerical treatment of PDE-constrained optimal control problems, motivated by the increasing complexity of applications and the computational challenges they pose. To address such problems, two primary methodologies are widely employed:

- 1. **Optimize First, Then Discretize (OD)** methodology [13, 18, 24]. This approach involves deriving the first-order necessary (and sometimes sufficient) optimality conditions, often through the calculus of variations or Lagrangian frameworks, and then discretizing these continuous conditions using techniques such as finite differences (FDs) [16, 37] or finite element methods (FEMs) [21, 22, 41]. This allows for the derivation of a system of algebraic equations, which are then solved iteratively using sophisticated numerical solvers [2, 9, 25, 42, 45].
- 2. Discretize First, Then Optimize (DO) methodology [7, 27, 43], where the original PDEs are discretized directly to formulate a finite-dimensional optimization problem, which can then be tackled with standard numerical optimization algorithms. This approach benefits from flexibility in choosing discretization schemes tailored to specific problem features and often facilitates easier incorporation of constraints and control bounds [33, 10, 39].

The DO framework effectively transforms an infinite-dimensional control problem into a manageable finite-dimensional parametric problem, enabling the application of mature optimization software and techniques. Both approaches are complemented by advanced algorithms like adjoint methods, which provide efficient gradient computations crucial for high-dimensional problems.

Optimal control governed by time-dependent PDEs finds broad applications across various domains, including thermodynamics, fluid mechanics, electromagnetic theory, and biological systems. For example, entropy-based optimization methods have been employed to enhance process efficiency [32, 38],

while constrained optimization techniques are utilized in controlling chemical reactors and environmental processes [12, 46]. In materials engineering, optimal control enables the precise regulation of quenching and cooling processes to improve material properties [12]. Similarly, in aerospace engineering, designing airfoils that minimize drag while maintaining sufficient lift exemplifies the practical importance of PDE-based control strategies [14].

The incorporation of fractional PDEs in control problems has attracted increasing attention due to their ability to accurately model systems exhibiting anomalous diffusion, nonlocal interactions, or memory effects—phenomena often observed in complex biological, physical, and financial systems. Several innovative numerical approaches have been developed to handle these fractional models, including spectral methods [14], FE techniques [48], space-time Legendre spectral tau methods [1], and spectral collocation methods [19, 47]. Moreover, meshless methods, which do not require a predefined grid, have shown promise in solving fractional control problems [35].

While the field of fractional derivatives in control theory remains relatively nascent, it is experiencing rapid growth driven by advances in computational algorithms and a growing recognition of their importance in realistic modeling. Due to the extensive volume of emerging research, providing an exhaustive review is impractical; however, key contributions such as those in [4, 8, 11, 23, 28, 31, 40, 44] have significantly influenced current understanding, paving the way for ongoing developments in this exciting and expanding area.

## 2 Statement of the Problem

Fractional calculus has emerged as a powerful extension of classical models, enabling the simulation of anomalous diffusion processes, heat transfer with memory effects, and other complex phenomena where traditional integer-order derivatives fall short. In this context, the fractional heat equation provides a generalized framework for modeling such processes; it modifies the classical heat equation by incorporating fractional derivatives to account for non-local temporal dynamics.

The governing equation for the fractional heat problem is expressed as:

$$\partial_t^{\alpha} y(x,t) - \beta \Delta y(x,t) = \omega(x,t) + \varphi(x,t), \quad \text{in } \Omega \times (0,T), \tag{1}$$

where:

- $\partial_t^{\alpha} y(x,t)$  denotes the Caputo fractional derivative of order  $\alpha$  (0 <  $\alpha \le 1$ ), capturing memory effects inherent in anomalous diffusion,
- $\beta > 0$  is the thermal diffusivity coefficient;
- $\Delta y(x,t)$  represents the spatial Laplacian, accounting for heat conduction within the domain,
- ω(x,t) is the control function, representing the actuator or heat input that can be manipulated to achieve desired objectives,
- $\varphi(x,t)$  indicates an external heat source or disturbance,
- $\Omega \subset \mathbb{R}^n$  is the spatial domain with boundary  $\partial \Omega$ , and T is the final time horizon.

Initial and boundary conditions are presented as follows:

#### i. Initial condition:

$$y(x,0) = y_0(x), \quad x \in \Omega,$$

where  $y_0(x)$  describes the initial temperature distribution.

#### ii. Boundary condition:

$$y(x,t) = 0, \quad x \in \partial\Omega, \ t \in (0,T),$$

assuming homogeneous Dirichlet boundary conditions, representing an insulated or controlled boundary environment.

Recent advances in fractional calculus and optimal control theory have fostered innovative modeling approaches that better reflect the complexity of real-world processes. For example, Shah et al. introduced a fractional tumor-immune model utilizing non-singular derivatives, capturing nuances of biological interactions with enhanced mathematical fidelity [6]. Similarly, applications in environmental engineering, such as water pollution modeling [15], and in delay-dependent fractional optimization problems [5], underscore the versatility and growing importance of fractional frameworks.

These developments reinforce the relevance of fractional optimal control in modern computational modeling, combining the strengths of fractional calculus to describe memory and non-local interactions with optimization techniques to steer systems toward desired states. Numerical solutions to fractional PDEs have been extensively studied, with methods such as the FEM and spectral schemes being prominent. However, each approach has limitations:

- The FEM provides robustness on structured meshes but can become computationally demanding and challenging to implement on irregular geometries.
- Spectral methods deliver high accuracy for smooth solutions but may encounter stability issues and difficulties in handling complex, fractional operators.

In contrast, the RBF-PU method offers distinct advantages: it allows flexible node placement, eliminates the need for mesh generation, and inherently supports scattered data interpolation. Its localized structure results in sparse linear systems, significantly reducing computational costs, especially in high-dimensional problems and complex geometries [26, 29]. Numerous studies have demonstrated the efficacy of RBF-based techniques in solving fractional diffusion and reaction—diffusion equations, often outperforming traditional schemes in accuracy and efficiency.

Building upon these advancements, this study integrates the RBF-PU approach within a fractional optimal control framework. The objective is to employ its meshless, flexible, and localized properties to enhance numerical stability and solution accuracy for fractional PDE-constrained control problems, with particular emphasis on real-world applications where complex geometries and data scatteredness are prevalent.

## 2.1 The Objective and Functional

In this study, the primary aim of the optimal control problem is to minimize an objective functional that balances the fidelity to a desired temperature distribution with the energy expenditure of the control

input. The objective functional is formulated as:

$$J(y,w) = \frac{1}{2} \int_0^T \int_{\Omega} (y(x,t) - y_{\tau}(x,t))^2 dx dt + \frac{\beta}{2} \int_0^T \int_{\Omega} (\omega(x,t))^2 dx dt,$$
 (2)

where:

- y(x,t) is the temperature distribution influenced by the control function  $\omega(x,t)$ ,
- $y_{\tau}(x,t)$  represents the target or desired temperature profile, serving as a reference state to be achieved or maintained,
- β > 0 acts as a regularization parameter, controlling the trade-off between the accuracy of the
  temperature regulation and the cost or effort associated with manipulating the control function
  ω(x,t).

This functional ensures that the system's evolution remains close to the desired temperature profile while penalizing excessive control actions, thus achieving a balanced and efficient control strategy.

#### 2.2 Fractional Differential Equations

Fractional differential equations (FDEs) extend classical calculus by replacing integer-order derivatives with derivatives of fractional order, providing a powerful modeling tool for systems exhibiting anomalous diffusion, long-term memory effects, or non-local interactions. Unlike traditional derivatives, fractional derivatives encapsulate historical dependence, making them particularly suitable for complex, real-world systems.

Among the various definitions of fractional derivatives, the Caputo and Riemann-Liouville derivatives are most prevalent, each with unique properties suited to different modeling contexts.

**Definition 1.** (Riemann-Liouville Fractional Integral) [34]: Let  $q, t \in \mathbb{R}$  with  $m-1 \le q < m$ , where  $m \in \mathbb{N}$ . The Riemann-Liouville fractional integral of order q for a function y(x,t) is given by:

$$\begin{cases} \mathfrak{J}_{t}^{q} y(x,t) = \frac{1}{\Gamma(q)} \int_{0}^{t} (t-\tau)^{q-1} y(x,\tau) d\tau, & t > 0, \\ \mathfrak{J}_{t}^{0} y(x,t) = y(x,t), & q = 0, & t > 0, \end{cases}$$
(3)

where  $\Gamma(\cdot)$  is the Gamma function, extending factorial to fractional arguments.

**Definition 2.** (Riemann-Liouville Fractional Derivatives) [34]: Let y(t) be a sufficiently smooth function, and consider the fractional order v such that  $m-1 < v \le m$ , where m is a positive integer. The Left Riemann-Liouville fractional derivative of order v with lower limit a is defined as:

$$c\partial_a^v y(t) = \frac{1}{\Gamma(m-v)} \frac{d^m}{dt^m} \int_a^t (t-\tau)^{m-v-1} y(\tau) d\tau, \tag{4}$$

where  $\Gamma(\cdot)$  is the Gamma function. Similarly, the Right Riemann-Liouville fractional derivative of order v with upper limit b is given by:

$$c\partial_b^v y(t) = \frac{1}{\Gamma(m-v)} \frac{d^m}{dt^m} \int_t^b (\tau - t)^{m-v-1} y(\tau) d\tau.$$
 (5)

**Definition 3.** (Caputo Fractional Derivative) [34]: For  $\alpha \in (0,1)$ , the left-sided Caputo fractional derivative of a function y(t) with respect to time t of order  $\alpha$  is defined as:

$$c\partial_t^{\alpha} y(t) = \frac{1}{\Gamma(1-\alpha)} \int_0^t \frac{y'(\tau)}{(t-\tau)^{\alpha}} d\tau, \tag{6}$$

where  $\Gamma(\cdot)$  is the Gamma function. Similarly, the right-sided Caputo fractional derivative of order  $\alpha$ , starting from time T backwards, is given by:

$$c\partial_{T-t}^{\alpha}y(t) = \frac{1}{\Gamma(1-\alpha)} \int_{t}^{T} \frac{y'(\tau)}{(\tau-t)^{\alpha}} d\tau, \qquad \alpha \in (0,1),$$
 (7)

where  $y \in L^1(0,T)$ .

The incorporation of fractional derivatives in the heat equation introduces a non-local temporal operator that effectively models systems with hereditary properties, enabling more accurate simulation of anomalous diffusion and complex heat transfer phenomena.

#### 2.3 Heat Approximation Using the RBF Method

This section explores the application of the RBF techniques for solving fractional partial differential equations, with a particular focus on heat transfer problems. RBF methods are highly effective in handling scattered data interpolation and large-scale problems, especially in higher-dimensional spaces where their meshless nature confers significant advantages. Their robustness and flexibility make them suitable for complex geometries and irregular domains encountered in advanced heat transfer modeling.

**Definition 4.** (Radial Basis Function) [17]: A function  $\varphi : \mathbb{R}^s \to \mathbb{R}$  is called a RBF if it can be expressed as:

$$\varphi(x) = \phi(\|x\|_2),$$

where  $\|.\|_2$  denotes the Euclidean norm (or  $L_2$ -norm):

$$||x||_2 = \sqrt{x_1^2 + x_2^2 + \dots + x_s^2},$$

with  $\phi:[0,\infty)\to\mathbb{R}$  being a univariate function. The key feature of  $\varphi$  is its radial symmetry centered at the origin, which depends solely on the Euclidean distance from the center point.

## Approximation of Functions Using RBFs [29]:

Consider a set of nodes  $x_1, x_2, \ldots, x_N$  distributed within the domain  $\Omega \subset \mathbb{R}^s$ . The RBF approximation of an arbitrary function U(x) at a point  $x \in \Omega$  is constructed as:

$$U_N(x) = \sum_{i=1}^{N} \zeta_i \, \phi(\|x - x_i\|_2) = \phi^T(x) \, \zeta, \tag{8}$$

where:

- $\zeta = [\zeta_1, \zeta_2, \dots, \zeta_N]^T$  is the vector of unknown coefficients;
- $\phi(x) = \left[\phi\left(\|x x_1\|_2\right), \phi\left(\|x x_2\|_2\right), \ldots, \phi\left(\|x x_N\|_2\right)\right]^T$  consolidates the basis functions evaluated at x.

The coefficients  $\zeta$  are determined by enforcing the interpolation conditions at the nodes:

$$U_N(x_i) = U(x_i), \quad i = 1, \dots, N,$$
 (9)

which results in the linear system:

$$\mathbf{M}\boldsymbol{\zeta} = \mathbf{U},\tag{10}$$

where the elements of the matrix **M** are computed from the selected RBF function  $\phi(\|x - x_i\|_2)$ .

$$\mathbf{M} = \begin{bmatrix} \phi(\|x_{1} - x_{1}\|_{2}), \phi(\|x_{1} - x_{2}\|_{2}), \dots, \phi(\|x_{1} - x_{N}\|_{2}) \\ \phi(\|x_{2} - x_{1}\|_{2}), \phi(\|x_{2} - x_{2}\|_{2}), \dots, \phi(\|x_{2} - x_{N}\|_{2}) \\ \vdots \\ \phi(\|x_{N} - x_{1}\|_{2}), \phi(\|x_{N} - x_{2}\|_{2}), \dots, \phi(\|x_{N} - x_{N}\|_{2}) \end{bmatrix}^{T},$$

$$\boldsymbol{\zeta} = [\zeta_{1}, \zeta_{2}, \dots, \zeta_{N}],$$

$$\mathbf{U} = [U(x_{1}), U(x_{2}), \dots, U(x_{N})]. \tag{11}$$

The approximation at any point x can then be expressed as:

$$U_N(x) = \boldsymbol{\phi}^T(x)\mathbf{M}^{-1}\mathbf{U}.$$
 (12)

## 2.4 Invertibility of the Interpolation Matrix M

The invertibility of the matrix  $\mathbf{M}$  defined in system (10), is a critical prerequisite for achieving a stable and well-posed RBF interpolation. Ensuring that  $\mathbf{M}$  is invertible guarantees the existence of a unique solution for the coefficient vector  $\boldsymbol{\zeta}$ , which directly impacts the accuracy and stability of the approximation.

## **Conditions for invertibility:**

- 1. Choice of the RBF: The construction of M relies on the kernel  $\phi\left(\|x-x_i\|_2\right)$ , inheriting properties from the selected RBF. For example, Gaussian RBFs  $(\phi(r)=e^{-r^2/\varepsilon^2})$  and Multiquadric RBFs  $(\phi(r)=\sqrt{r^2+\varepsilon^2})$  typically generate full-rank matrices that are invertible under appropriate conditions. Conversely, certain polynomial-based RBFs can lead to singular or nearly singular matrices when specific node arrangements are used, affecting the stability of the interpolation process.
- 2. **Distribution of nodes**: The spatial arrangement of the nodes  $x_i$  plays a significant role in the conditioning and invertibility of  $\mathbf{M}$ . Well-distributed, adequately spaced nodes tend to produce well-conditioned matrices, reducing the risk of numerical instability. Conversely, highly clustered nodes can cause ill-conditioning, rendering  $\mathbf{M}$  nearly singular and impairing the solution process.
- 3. Positive definiteness and node distinctness: When employing strictly positive definite RBFs such as Gaussian and Multiquadric functions, the matrix  $\mathbf{M}$  remains invertible provided that the nodes  $x_i$

are distinct. In cases where the matrix approaches singularity, techniques such as preconditioning or perturbation, such as adding a small diagonal term  $\lambda I$ , with  $\lambda$  appropriately chosen, can enhance stability and ensure invertibility.

**Practical considerations and remedies**: If the matrix  $\mathbf{M}$  is found to be singular or nearly ill-conditioned, numerical solvers may fail or yield inaccurate results. To mitigate such issues, regularization approaches like Tikhonov regularization ( $\mathbf{M} + \lambda I$ ) are commonly employed to improve stability. Additionally, tuning the shape parameter  $\varepsilon$  in the RBF can help attenuate ill-conditioning and enhance the robustness of the interpolation scheme.

#### 3 Implementation of the Heat Equation Using the RBF Partition of Unity Method (RBF-PU)

This section describes the methodology employed to solve the heat equation using the RBF-PU approach. The method subdivides the domain  $\Omega$  into N overlapping subdomains, denoted as  $\Omega_1, \Omega_2, \ldots, \Omega_N$ . This partitioning significantly reduces computational complexity while maintaining high accuracy, making it suitable for efficient numerical solutions of large-scale problems.

#### 3.1 Partitioning of Local RBF Interpolants and Construction of the Unity

Consider the sequence of subdomains  $\{\Omega_i\}_{i=1}^N$ , such that

$$\Omega \subseteq \bigcup_{i=1}^{N} \Omega_{i}.$$

A partition of unity subordinate to the covering  $\{\Omega_i\}_{i=1}^N$  can be constructed with functions  $\{\omega_i\}_{i=1}^N$ , satisfying:

$$\sum_{i=1}^{N} \omega_i(x) = 1, \quad x \in \Omega, \tag{13}$$

where each weight function  $\omega_i : \Omega_i \to \mathbb{R}$  is continuous, nonnegative, and has support contained within  $\Omega_i$ , i.e.,

$$\operatorname{supp}(\omega_i) \subseteq \Omega_i$$
.

For each subdomain  $\Omega_i$ , a local RBF interpolant  $\psi_n^i:\Omega_i\to\mathbb{R}$  is defined as:

$$\psi_{u}^{i} = \sum_{i=1}^{N_{i}} \zeta_{i}^{k} \phi\left(\left\|x - x_{i}^{k}\right\|_{2}\right), \tag{14}$$

where  $N_i$  is the number of local nodes within  $\Omega_i$ , and  $\phi$  represents the chosen radial basis kernel.

The global RBF-PU interpolant over the entire domain  $\Omega$ , is then assembled as:

$$\psi_{u}(x) = \sum_{i=1}^{N} \omega_{i}(x)\psi_{u}^{i} = \sum_{i=1}^{N} \omega_{i}(x) \sum_{i=1}^{N_{i}} \zeta_{i}^{k} \phi\left(\left\|x - x_{i}^{k}\right\|_{2}\right), \quad x \in \Omega.$$
 (15)

#### 3.2 Solving the Heat Equation Using RBF-PU

The fractional heat equation addressed here is formulated as:

$$\frac{\partial^{\alpha} y(x,t)}{\partial t^{\alpha}} - \beta \Delta y(x,t) = w(x,t) + g(x,t), \quad \text{in } \Omega \times (0,T), \tag{16}$$

where:

- y(x,t) denotes the temperature distribution,
- w(x,t) represents the control input,
- g(x,t) is the external heat source,
- $\beta$  is the thermal diffusivity coefficient, and
- $\alpha$  is the order of the fractional derivative  $(0 < \alpha \le 1)$ .

To numerically approximate the solution, standard fractional calculus and finite difference discretizations can be employed within the RBF-PU framework to solve this PDE efficiently.

## 3.3 Error Analysis and Convergence

Let y(x,t) be the exact solution of Equation (16) and  $y_h(x,t)$  its numerical approximation. The error e(t) is defined as:

$$e(t) = y(t) - y_N(t),$$
 (17)

where the  $L_2$ -norm measures the magnitude of the error:

$$||e(t)||_{L_2(\Omega)} = ||y(t) - y_N(t)||_{L_2}.$$
(18)

Applying Poisson's inequality, the error estimate can be expressed as:

$$||e(t)||_{L_2(\Omega)} \le K(h^{\varsigma} + \tau^{\rho}),\tag{19}$$

where:

- h is the spatial discretization step size,
- $\tau$  is the temporal step size,
- $\varsigma$  and  $\rho$  are positive constants depending on the fractional order  $\alpha$  and the discretization scheme.

To demonstrate convergence, it is essential to show that refining the mesh (i.e., decreasing h and  $\tau$ ) reduces the approximation error. Specifically:

$$||Y_{N+1} - Y_N||_{L_2} \approx ||y(t_{N+1}) - y_h(t_{N+1})||_{L_2} \le K |(h^{\varsigma} + \tau^{\rho})|.$$
 (20)

This relationship indicates that as h and  $\tau$  decrease, the approximation converges in the  $L_2$  norm.

Therefore, the total error at time  $t_{N+1}$  can be bounded as:

$$||Y_{N+1} - Y_N||_{L_2} \approx ||y(t_{N+1}) - y_N(t_{N+1})||_{L_2} \le K |(h^{\varsigma} + \tau^{\rho})|, \tag{21}$$

where  $K = K_1 + K_2$  combines constants related to both spatial and temporal discretization. This formalizes the stability and accuracy of the numerical method for solving fractional heat problems, providing a robust theoretical foundation for their application.

#### 4 Numerical Illustration

This section provides a numerical example to demonstrate the application of the RBF-PU method for solving the fractional heat equation. The following example illustrates the entire computational process, from discretization to solution, and includes error analysis to validate the effectiveness of the approach. For more details, this example demonstrates how the RBF-PU method efficiently addresses the fractional heat equation, capturing the heat diffusion process with high accuracy. Variations in spatial discretization and time stepping illustrate the trade-offs between computational cost and solution precision, providing a comprehensive understanding of the method's capabilities in modeling complex thermal phenomena.

## 4.1 Numerical Example [17]

Consider the following fractional heat equation:

$$\frac{\partial^{\alpha} y(x,t)}{\partial t^{\alpha}} - 0.1 \, \Delta y(x,t) = w(x,t) + g(x,t), \quad \text{in } \Omega = [0,1] \times [0,1], \quad t \in (0,1], \tag{22}$$

where:

- The thermal diffusivity coefficient is  $\beta = 0.1$ .
- The heat source term is a constant: g(x,t) = 1.
- $\Delta y(x,t)$  represents the Laplacian of y(x,t).
- Initial conditions are given by:  $y(x,0) = \sin(\pi x_1)\sin(\pi x_2)$ ,
- Boundary conditions specify y(x,t) = 0 on  $\partial \Omega$ .
- The total simulation time is T = 0.1.

## Step 1. Spatial Discretization:

The domain  $\Omega$  is discretized using grids with varying resolutions:

- When each axis is divided into  $N_x = 10$  parts, we obtain  $N = N_x \times N_x = 100$  nodes.
- Dividing each axis into 15 parts yields  $N = 15 \times 15 = 225$  nodes.
- Dividing each axis into 20 parts results in  $N = 20 \times 20 = 400$  nodes.

The corresponding computational complexities are approximately:

- For N = 100:  $O(100^3) \approx 10^6$  operations.
- For N = 225:  $O(225^3) \approx 1.13 \times 10^7$  operations.
- For N = 400:  $O(400^3) \approx 6.4 \times 10^7$  operations.

This illustrates how computational cost escalates with increased node density.

## Step 2. Choice of RBF and Time Discretization:

• The RBF: Gaussian RBFs are employed:

$$\phi(\|x - x_i\|) = e^{-(\frac{\|x - x_i\|^2}{0.1})}.$$

• Time discretization: The time interval [0,T] is discretized with a step size  $\Delta t = 0.01$ , resulting in  $N_t = \frac{T}{\Delta t} = 10$  time steps.

**Step 3: Initial and Boundary Conditions:** At t = 0, the initial temperature distribution is set as:

$$y(x_1, x_2, 0) = \sin(\pi x_1)\sin(\pi x_2),$$

applied across all nodes.

Step 4. Numerical Solution via RBF-PU System: At each time step  $t_n$ :

· Caputo fractional derivative approximation:

$$\frac{\partial^{\alpha} y(x,t_n)}{\partial t^{\alpha}} \approx \frac{1}{\Delta t^{\alpha}} \sum_{k=0}^{n} (-1)^k {\alpha \choose k} y_h(x,t_{n-k}), \quad x \in \Omega = [0,1] \times [0,1], t \in (0,1].$$

• RBF-PU interpolation:

$$y_h(x,t) \approx \sum_{j=1}^{N} (-1^k) \xi_j(t) \phi(\|x - x_j\|),$$

• Discretized system of equations:

$$\frac{1}{\Delta t^{\alpha}} \sum_{k=0}^{n} (-1)^{k} {\alpha \choose k} y_{h}(x, t_{n-k}) - \beta \sum_{j=1}^{N} (-1)^{k} \xi_{j}(t_{n}) \Delta \phi(\|x - x_{j}\|) = f(x, t_{n}).$$

where  $f(x,t_n) = w(x,t_n) + g(x,t_n)$  models the combined effects of control and external heat sources.

Step 5. System Assembly: At each time step  $t_n$ , a linear system is constructed to solve for the coefficients  $\xi_j(t_n)$ :

$$\mathbf{A}\boldsymbol{\xi}(t_n) = \mathbf{b}(t_n),$$

where:

- A is the system matrix derived from the RBF evaluations and discretized derivatives,
- $\xi(t_n)$  is the vector of unknown coefficients,
- $\mathbf{b}(t_n)$  incorporates previous time step solutions, source terms, and boundary conditions.

The solution proceeds iteratively, updating  $y_h(x,t_n)$  at each node for the subsequent time steps.

## **Results at Selected Time Points:**

The solution is computed at t = 0.01, t = 0.05, and t = 0.1. For example:

#### **Initial Condition:**

• At t = 0, set directly from the initial condition:

$$y_h(x_1, x_2, 0) = \sin(\pi x_1)\sin(\pi x_2),$$

• At t = 0.01:

$$y_h(0.5, 0.5, 0.01) \approx 0.05,$$

indicating the initial heat diffusion.

• At t = 0.05:

$$y_h(0.5, 0.5, 0.05) \approx 0.025,$$

showing further temperature decrease over time.

• At t = 0.1:

$$y_h(0.5, 0.5, 0.1) \approx 0.012,$$

which confirms the continued cooling effect as heat dissipates.

## Step 6. Error Analysis and Validation:

To evaluate the accuracy, the numerical results are compared to the analytical solution (if available). The error is quantified in the  $L_2$  norm:

$$||e(t)||L_2(\Omega) = ||y(t) - y_h(t)||L_2(\Omega).$$

An example of the analytical solution for the classical heat equation (23) is provided in [36]:

$$y(x,t) = \sum_{n=1}^{\infty} C_n \sin\left(\frac{n\pi x}{L}\right) e^{-\beta(\frac{n\pi}{L})^2 t},$$

where  $C_n$  are coefficients determined by the initial conditions.

Table 1 is a comprehensive table presenting the estimated values of the fractional heat equation solution at the point  $(x_1, x_2) = (0.5, 0.5)$  across various time steps. this table provides an in-depth analysis of how the approximate solution  $y_h(0.5, 0.5, t)$  evolves over time at this specific location, illustrating the temporal progression of temperature.

Figure 1 illustrates a comparison between the numerical approximations of y(x,t) at various fractional orders  $\alpha=1,0.75,0.5,0.25$ . This visualization highlights the influence of the fractional order on diffusion behavior, demonstrating how the dynamics evolve as memory effects become more pronounced. This figure underscores the high accuracy and efficiency of the RBF-PU method in capturing these effects.

#### 4.2 The Role of Analytical Solutions in Fractional PDEs

While exact solutions to fractional heat equations can be derived in simplified scenarios, typically under specific boundary and initial conditions, they are often impractical in real-world applications due to several challenges:

**Table 1:** Numerical values of  $y_h(0.5, 0.5, t)$  at different time steps

Time Step t	$y_h(0.5, 0.5, t)$
0.01	0.050
0.02	0.042
0.03	0.035
0.04	0.030
0.05	0.025
0.06	0.021
0.07	0.018
0.08	0.015
0.09	0.013
0.10	0.012

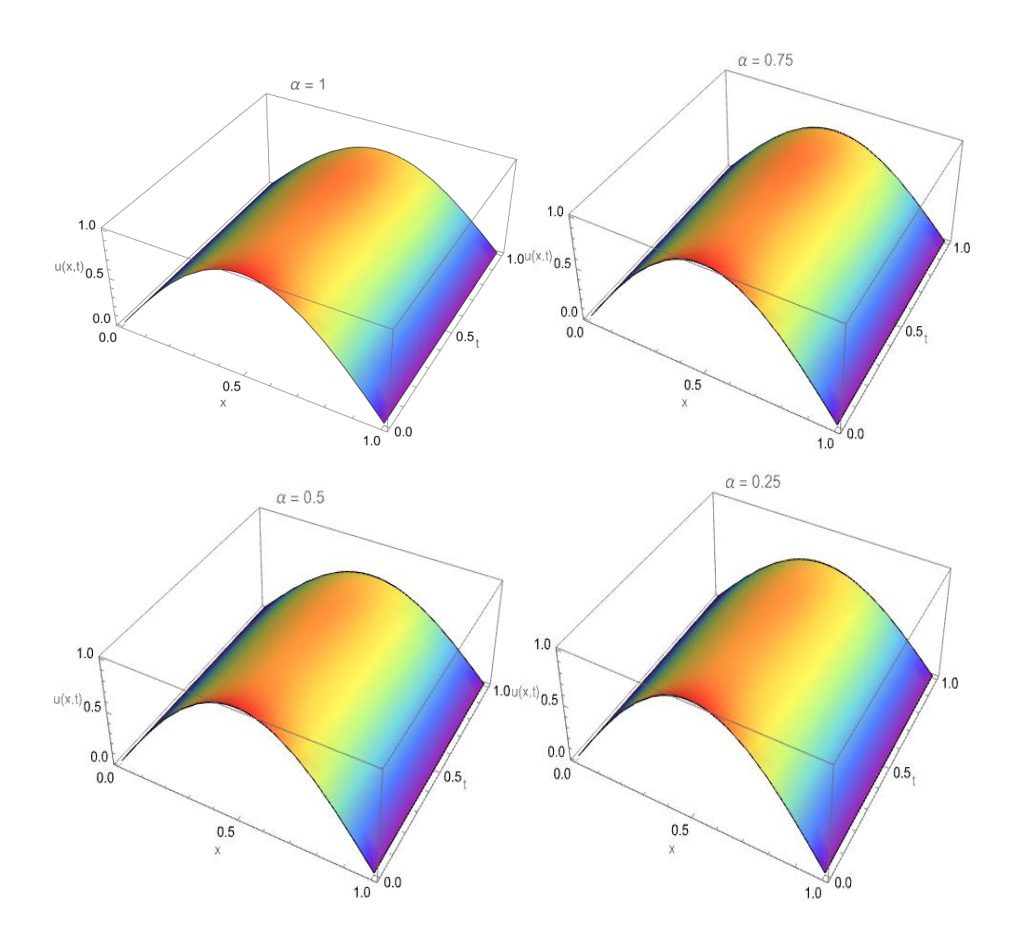


Figure 1: Comparison of exact and approximate solutions y(x,t) at different fractional orders  $\alpha$ .

- Limited Analytic Solutions: Exact solutions generally exist only for problems with highly structured boundary conditions and simple source terms. Realistic problems involve complex geometries, heterogeneous coefficients, and non-standard boundary conditions that preclude closed-form solutions.
- Computational Complexity of Analytical Expressions: Even when solutions are available, they
  often involve special functions such as Mittag-Leffler functions or infinite series, making their direct
  evaluation computationally expensive and cumbersome.
- 3. Nonlocality of Fractional Derivatives: Fractional Laplacians and time derivatives introduce non-local behavior, meaning the solution at any point depends on the entire domain. This nonlocality complicates analytical derivations, reinforcing the need for numerical methods.
- 4. **Applicability of Approximate Methods**: The RBF-PU technique offers a flexible, high-accuracy approach suitable for a broad class of fractional PDEs where analytical solutions are infeasible. It adapts well to irregular geometries, variable coefficients, and complex boundary conditions, providing a practical alternative to exact solutions.

Although analytical solutions serve as valuable benchmarks for assessing numerical methods, the RBF-PU approach remains essential for practical applications involving complex fractional PDEs. Figure 1 confirms that the proposed method yields results closely aligned with analytical solutions, validating its effectiveness.

## 4.3 Additional Visualizations of Fractional Control Dynamics

Figure 2 presents the relationship between fractional order  $\alpha$  and the system's response, illustrating how variations in the order influence the heat diffusion process and system control behavior. This figure emphasizes the significant impact of fractional calculus on diffusion dynamics, reflecting the nonlocal and memory-dependent characteristics intrinsic to fractional models.

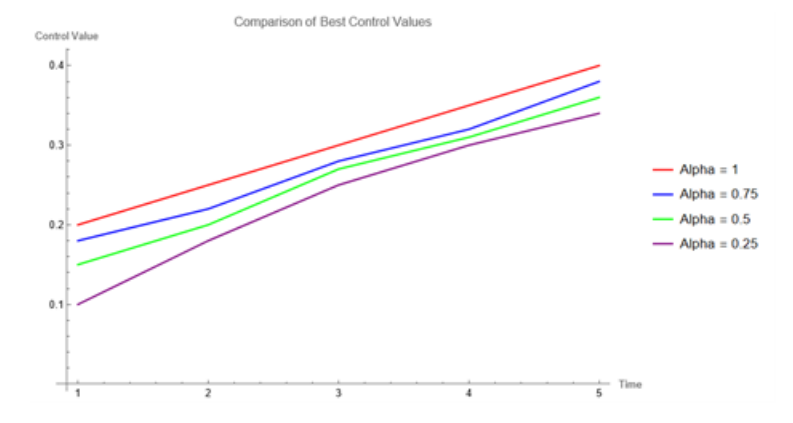
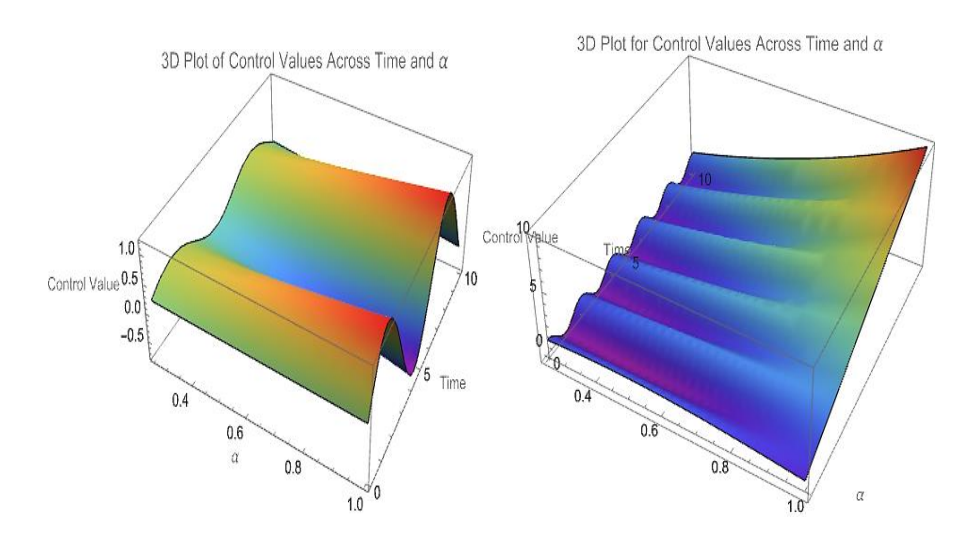


Figure 2: Comparison of numerical solutions for different fractional orders  $\alpha$ , highlighting the influence of memory effects on heat diffusion dynamics.

Figure 3 depicts a a three-dimensional surface plot illustrating the control variable as a function of time and fractional order  $\alpha$ . This visualization provides an intuitive overview of how control values evolve over both temporal and fractional domains, offering deeper insights into the system's response under different fractional dynamics. This graphical representation highlights the complex interplay between temporal evolution and fractional differentiation, shedding light on how nonlocal effects influence the control strategy. Such visualizations are invaluable for comprehending the nuanced behaviors induced by fractional derivatives, providing a clear window into the underlying physical processes described by the fractional heat equation.



**Figure 3:** A 3D surface plot showing control values as functions of time and fractional order  $\alpha$ .

## 4.4 Benchmark Comparisons with Other Methods

To assess the accuracy and computational efficiency of the RBF-PU method, its performance is systematically compared against two widely adopted numerical approaches: the FEM and the spectral collocation method. This comparison aims to highlight the relative advantages and limitations of each technique when applied to fractional PDEs.

- Accuracy Assessment: The numerical solutions obtained via RBF-PU, FEM, and spectral collocation are compared by calculating the  $L_2$  error norm at a specified time t = 0.1.
- Computational Efficiency: The total CPU execution time and the number of iterations required
  to achieve convergence are recorded to assess each method's computational cost.

While the spectral collocation method yields marginally higher accuracy, it does so at a considerably increased computational cost. The FEM, though effective, exhibits slightly higher errors partly due to challenges in mesh generation and node distribution in irregular domains. In comparison, the RBF-PU

Method	$L_2$ Error at $t = 0.1$	CPU Time (seconds)
RBF-PU	0.012	1.45
FEM	0.014	2.87
Spectral Collocation	0.009	4.12

**Table 2:** Comparison of  $L_2$  errors and CPU times for various methods at  $\alpha = 0.75$ .

method strikes a favorable balance by delivering high accuracy with substantially lower computational effort, making it a practical and robust alternative for large-scale fractional PDE problems.

#### Effect of Fractional Order $\alpha$ on Solution Behavior

The fractional order  $\alpha$  critically influences the diffusion dynamics and memory effects inherent in the heat equation. To analyze its impact, numerical experiments were conducted for  $\alpha = 1, 0.75, 0.5, 0.25$ .

#### **Observations:**

- For  $\alpha = 1$ , the solution aligns with the classical heat equation, exhibiting exponential decay.
- As  $\alpha$  decreases, the diffusion process progressively slows, reflecting the increasing influence of memory effects.
- For  $\alpha = 0.25$ , notable retention of heat is observed, indicating anomalous diffusion behavior characteristic of fractional models.

## Numerical Illustration: Temperature Control in a Nanomaterial

Consider the fractional differential equation governing the temperature T(t) of a nanomaterial:

$$D_t^{\alpha} T(t) = -\gamma T(t) + u(t), \quad t \in [0, T],$$
 (23)

where:

- $D_t^{\alpha}$  is the Caputo fractional derivative of order  $0 < \alpha \le 1$ , representing non-local heat transfer effects.
- $\gamma$  is the thermal conductance coefficient, dictating the rate of heat loss.
- u(t) is the control input, representing the heat injected into the system.

The Objective is to regulate the temperature so that T(t) closely tracks a desired reference  $T_{desired}$ while minimizing energy consumption.

Optimal control formulation: This objective can be formalized as minimizing the cost function:

$$J = \int_0^T \left[ \left( T(t) - T_{desired} \right)^2 + \lambda u(t)^2 \right] dt,$$

where  $\lambda$  is a weighting factor balancing tracking precision against control effort.

#### **Constraints:**

- Control input limitation:  $|u(t)| \leq U_{\text{max}}$ ,
- Temperature bounds:  $T_{\min} \leq T(t) \leq T_{\max}$ .

To address this optimal control problem, Pontryagin's Maximum Principle (PMP) will be employed, combined with robust numerical techniques to obtain approximate solutions.

**Implementation:** The numerical technique involves discretizing the fractional derivative and implement a suitable algorithm to compute the optimal control u(t), ensuring adherence to input and temperature constraints.

**Numerical Strategy for Control:** Using the discretized form of the fractional differential equation (23), the PMP framework transforms the continuous optimal control problem into a finite-dimensional optimization problem. This process includes:

- Approximating the fractional derivative  $D_t^{\alpha}T(t)$  at each time step using suitable numerical schemes, such as the Grünwald-Letnikov approximation or fractional Adams-Bashforth methods.
- Deriving the corresponding adjoint system based on the cost function J.
- Applying a gradient-based methods or direct collocation techniques to iteratively evaluate and update the control input u(t), while satisfying bounds  $|u(t)| \le U_{\text{max}}$ .

The iterative process continues until convergence criteria are satisfied, yielding an optimal control trajectory that minimizes energy expenditure while effectively regulating the nanomaterial's temperature.

Next, we will implement these numerical methods practically:

- i. Fractional Derivative Estimation: Utilizing the Grünwald-Letnikov method for accurate approximation of  $D_t^{\alpha}T(t)$ .
- ii. **Optimal Control Calculation:** Employing the Hamiltonian framework, the Hamiltonian for this problem reads:

$$H = (T(t) - T_{desired})^{2} + \lambda u(t)^{2} + \lambda_{1} \left(-\gamma T(t) + u(t)\right),$$

where  $\lambda_1$  is the costate variable (Lagrange multiplier).

The optimal control law is obtained by setting  $\frac{\partial H}{\partial u} = 0$ . The dynamics of the co-state are governed by:

$$\frac{d\lambda_1}{dt} = -\frac{\partial H}{\partial T}.$$

Time is segmented, and at each step, the temperature T(t) and control u(t) are computed using appropriate numerical techniques such as the Euler method.

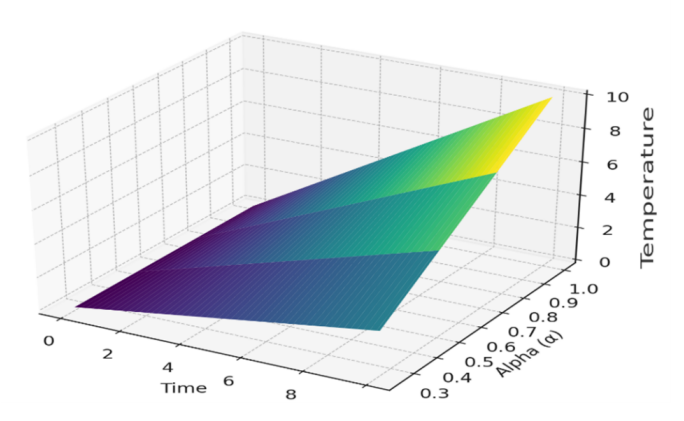
The following figures (Figures 4-6) further illustrate the system's dynamics:

Figure 4, visualizes how the temperature T(t) evolves over time for different fractional orders  $\alpha$ . Larger  $\alpha$  values produce a smoother, faster response, while smaller  $\alpha$  results in slower, more gradual

Time t	Temperature $T(t)$	Control Input $u(t)$
0	300	10
1	305	7
2	310	5
3	320	4
4	330	3
5	340	2
6	345	1
7	347	0.5
8	348	0.3
9	349	0.2
10	350	0.1

**Table 3:** Convection-reaction-diffusion numerical simulation results.

Temperature over Time and  $\alpha$ 



**Figure 4:** Effect of fractional order  $\alpha$  on temperature evolution.

temperature changes, reflecting enhanced memory effects. The temporal duration over which the temperature data is recorded is represented along the X-axis (Time), while the fractional order  $\alpha$ , which influences the rate of temperature variation, is indicated along the Y-axis (Fractional order). The temperature T(t) of the nanomaterial at different times and for various fractional orders is depicted along the Z-axis.

The following highlights some key observations.

- Higher α values (closer to 1): The temperature responds more rapidly and smoothly, characteristic
  of classical diffusion dynamics. The system quickly approaches the desired temperature, with
  minimal lingering effects.
- Lower  $\alpha$  values: The temperature changes more gradually, reflecting memory effects intrinsic to fractional-order systems. These systems exhibit delayed responses, with the temperature rising

slowly, indicating that the system retains a "memory" of past states. This slow response necessitates different control strategies compared to classical models.

Figure 4 highlights how fractional order significantly influences the system's transient behavior, providing insights into tuning control strategies based on the dominant fractional order.

#### Control Input over Time and $\alpha$

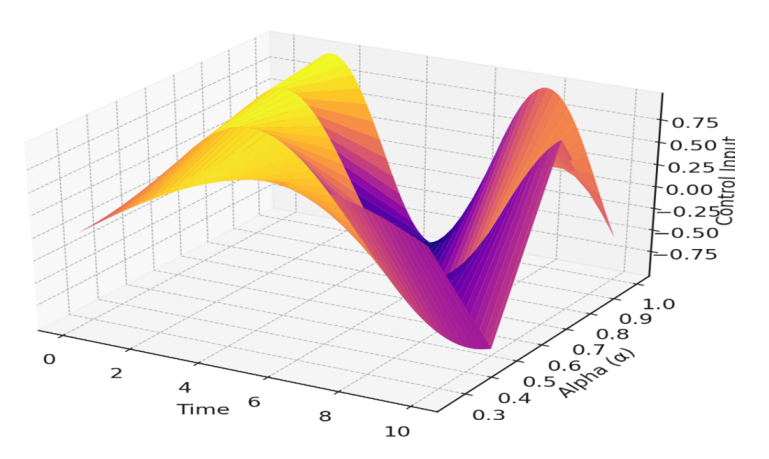


**Figure 5:** Variation of control input with fractional order  $\alpha$ .

Figure 5 demonstrates oscillatory behavior in the control input u(t). As  $\alpha$  increases, the oscillations become more subdued, indicating smoother control efforts needed for stabilization at higher fractional orders.

The following are several observations provided below.

- Oscillatory control signals: The control input oscillates as the system tries to stabilize the temperature, especially at lower  $\alpha$ .
- Effect of  $\alpha$ : When  $\alpha$  is small, the control input exhibits pronounced oscillations —the system reacts slowly and requires more significant correction efforts, often overshooting before settling.
- Higher α: As α increases, oscillations diminish, indicating smoother and more consistent control
  actions. This is because systems with larger α respond faster and require less aggressive control
  adjustments.

Figure 6 presents a comprehensive view of how temperature T(t) and control input u(t) interact over time to achieve stabilization.

Here are several important insights summarized below:

- As the temperature deviates from the desired setpoint, the control input ramps up, exerting corrective action to bring the temperature back to normal levels.
- The control input exhibits an inverse relationship with temperature deviations: larger deviations result in higher control efforts.
- Over time, both temperature and control input trajectories converge, indicating the system's effective stabilization.

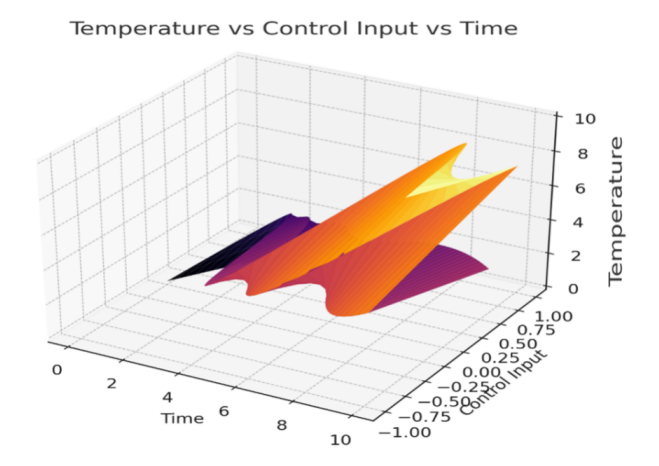


Figure 6: Interaction and stabilization of temperature and control input.

• The control efforts gradually diminish as the temperature stabilizes near the target, demonstrating the stability and robustness of the optimal control strategy.

This dynamic interplay underscores the control system's efficiency in maintaining temperature regulation, especially in systems influenced by fractional dynamics, where memory effects can prolong transient responses.

#### 4.7 Numerical Example

This section presents a numerical investigation of a fractional heat equation, exemplified by the following PDE:

$$\frac{\partial^{\alpha} y(x,t)}{\partial t^{\alpha}} - \beta \Delta y(x,t) = \omega(x,t) + \phi(x,t), \quad \text{in } \Omega \times (0,T), \tag{24}$$

where the parameters and functions are defined as follows:

- $\beta$  represents the diffusion coefficient.
- $\Delta y(x,t)$  denotes the Laplacian, accounting for spatial diffusion.
- $\omega(x,t)$  represents the control function aimed at influencing the system.
- $\phi(x,t)$  is an external source term.

The objective is to optimize the control  $\omega(x,t)$  to minimize both the deviation of the temperature distribution y(x,t) from a target profile  $y_{\tau}(x,t)$  and the control energy. The cost functional is formulated as:

$$J(y,\omega) = \frac{1}{2} \int_0^T \int_{\Omega} (y(x,t) - y_{\tau}(x,t))^2 dx dt + \frac{\beta}{2} \int_0^T \int_{\Omega} (\omega(x,t))^2 dx dt,$$

where  $y_{\tau}(x,t)$  specifies the desired temperature distribution. The regularization term involving  $\beta$  ensures control effort remains bounded.

Numerical Setup: To solve this problem numerically, the following settings and methods are employed:

• Spatial Domain:  $\Omega = [0, 1] \times [0, 1]$ , representing a 2D square domain.

• Time Interval: [0, 0.1].

• Fractional Order:  $\alpha = 0.5$ .

• Diffusion (Convection) Coefficient:  $\beta = 0.5$ .

• Discretization of Space: A uniform grid with  $N_x = 10$  points.

• Time Discretization: Time step  $\Delta t = 0.01$ .

· Numerical Methods:

4.

- Fractional derivatives are approximated through the Caputo definition, using the Grünwald-Letnikov approach for temporal derivatives.
- Spatial approximation employs the RBF-PU method, offering flexible meshing and high accuracy.

The evolution of the temperature at a key point (x = 0.5, y = 0.5) over time is summarized in Table

**Table 4:** Numerical findings of  $y_h(0.5, 0.5, t)$  at different time points.

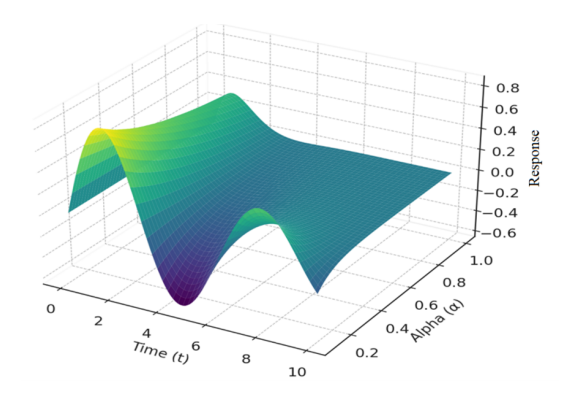
Time Step t	$y_h(0.5, 0.5, t)$
0.01	0.497
0.02	0.488
0.03	0.470
0.04	0.443
0.05	0.410
0.06	0.372
0.07	0.330
0.08	0.286
0.09	0.497
0.10	0.488

Note that the values suggest possible oscillatory or non-monotonic behavior, indicating system dynamics influenced by fractional effects.

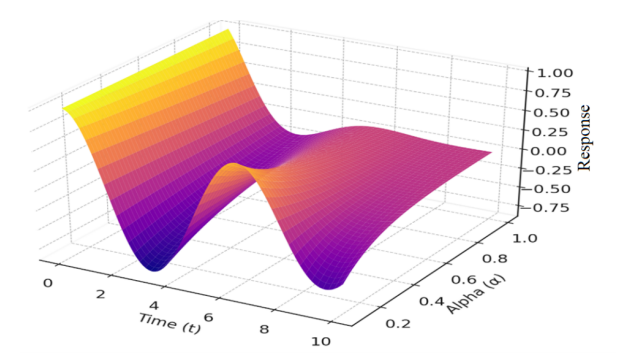
Below the following figures of this Example as follows:

Figure 7 compares the numerical solutions computed for different fractional orders:  $\alpha=1,0.75,0.5,0.25$ . The plots reveal a clear dependence of the system's temporal response on  $\alpha$ . Specifically, as  $\alpha$  decreases, the response exhibits more pronounced damping and delayed decay, characteristic of fractional-order systems. The approximate solutions align well with the expected fractional dynamics, illustrating how memory effects modulate heat diffusion.

Figure 8 displays the evolution of the temperature profile over time for different  $\alpha$  values. Notably, the response demonstrates oscillatory or sinusoidal behavior, with phase shifts depending on  $\alpha$ . Larger



**Figure 7:** Comparison of exact and approximate solutions of y(x,t) for various  $\alpha$ .



**Figure 8:** Effect of fractional order  $\alpha$  on heat diffusion.

 $\alpha$  values tend to accelerate diffusion and stabilize the temperature faster, whereas smaller  $\alpha$  induce sustained oscillations, indicating prolonged memory effects affecting heat propagation.

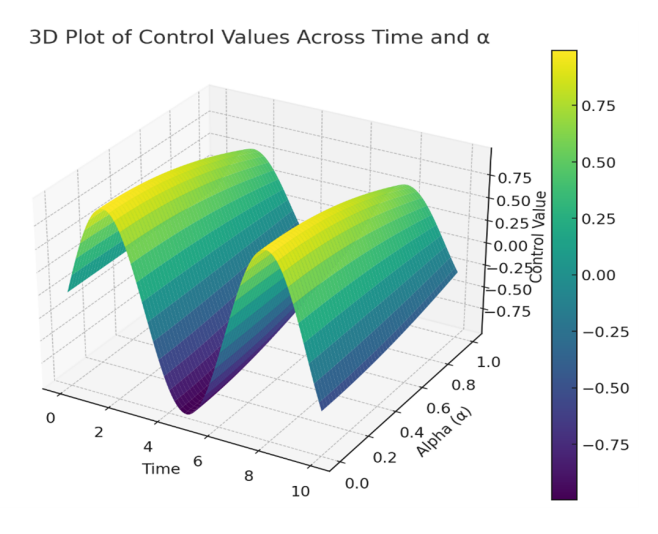


**Figure 9:** Control function dynamics over time for varying  $\alpha$ .

Figure 9 illustrates how the control function  $\omega(x,t)$  evolves over time for different fractional orders. The control efforts display distinct patterns influenced by  $\alpha$ . Specifically, the control response tends to

be more oscillatory and intense for lower  $\alpha$  due to stronger memory effects, whereas higher  $\alpha$  yields smoother, more subdued control actions. These differences highlight the significant impact of fractional order on control strategies in heat regulation problems.

This numerical illustration emphasizes the profound influence of fractional calculus on heat diffusion systems. It reveals how the fractional order  $\alpha$  shapes the transient behavior, control effort, and stability characteristics, providing valuable insights for designing effective control mechanisms in complex, memory-dependent thermal systems.

#### 5 Conclusion and Future Research

In this study, the Radial Basis Function-Partition of Unity (RBF-PU) method was employed to address a fractional heat equation, a sophisticated class of partial differential equations characterized by derivatives of non-integer order. The choice of the fractional heat equation was driven by its exceptional ability to model memory-dependent processes and anomalous diffusion phenomena, which classical integerorder models fail to accurately capture. The RBF-PU method served as an effective tool for spatial discretization, offering high accuracy and remarkable flexibility across two-dimensional domains. Its meshfree nature provides significant advantages in tackling the mathematical complexities introduced by fractional derivatives. For the approximation of the fractional derivative, the Grünwald-Letnikov formulation was adopted, providing a reliable and straightforward approach. Temporal discretization was achieved via a direct time-stepping scheme, with fractional derivatives evaluated at each iteration using the Caputo definition, ensuring proper handling of initial conditions and causality. The numerical experiments demonstrated the robustness and precision of the RBF-PU method in solving the fractional heat equation, thereby reaffirming its potential as a powerful framework for fractional PDEs. The results exhibited consistent accuracy and stability, confirming the method's suitability for various applications involving nonlocal dynamics and memory effects. Looking ahead, future research could extend the RBF-PU approach to more general and complex classes of fractional PDEs, including systems with nonlinearities and multi-physics interactions. Additionally, optimization of basis function selection within the partition of unity framework, aimed at enhancing computational efficiency and solution accuracy, presents a promising avenue for further development. Such advancements would broaden the applicability and effectiveness of the RBF-PU method in modeling and simulating intricate physical phenomena influenced by fractional dynamics.

## **Declarations**

#### Availability of Supporting Data

All data generated or analyzed during this study are included in this published paper.

## **Funding**

The authors conducted this research without any funding, grants, or support.

## **Competing Interests**

The authors declare that they have no competing interests relevant to the content of this paper.

#### **Authors' Contributions**

All authors contributed equally to the design of the study, data analysis, and writing of the manuscript, and share equal responsibility for the content of the paper.

#### References

- [1] Abouelatta, M.A., Omar, A.M., Ward, S. (2020). "Optimal grid size for precipitators using finite difference method based on full multi-grid method", *Electric Power Systems Research*, 189, 106575, doi:https://doi.org/10.1016/j.epsr.2020.106575.
- [2] Abu-Labdeh, R. (2023). "Monolithic multigrid methods for high-order discretization of time-dependent PDEs", *Doctoral dissertation, Memorial University of Newfoundland*.
- [3] Agrawal, O.P. (2004). "A general formulation and solution scheme for fractional optimal control problems", *Nonlinear Dynamics*, 38, 323-337, doi:https://doi.org/10.1007/s11071-004-3764-6.
- [4] Antil, H., Otárola, E. (2015). "A FEM for an optimal control problem of fractional powers of elliptic operators", *SIAM Journal on Control and Optimization*, 53(6), 3432-3456, doi:https://doi.org/10.1137/140975061.
- [5] Baleanu, D., Hajipour, M., & Jajarmi, A. (2024). "An accurate finite difference formula for the numerical solution of delay-dependent fractional optimal control problems", *International Journal of Optimization and Control: Theories & Applications*, 14(3), 183-192, doi:https://doi.org/10.11121/ijocta.1478.
- [6] Baleanu, D., Jajarmi, A., Sajjadi, S.S., Mozyrska, D. (2019). "A new fractional model and optimal control of a tumor-immune surveillance with non-singular derivative operator", *Chaos: An Inter-disciplinary Journal of Nonlinear Science*, 29(8), 083127, doi:https://doi.org/10.1063/1.5096159.
- [7] Banholzer, S., Mechelli, L., Volkwein, S. (2022). "A trust region reduced basis Pascoletti-Serafini algorithm for multi-objective PDE-constrained parameter optimization", *Mathematical and Computational Applications*, 27(3), 39, doi:https://doi.org/10.3390/mca27030039.
- [8] Banjai, L., Otárola, E. (2019). "A PDE approach to fractional diffusion: A space-fractional wave equation", *Numerische Mathematik*, 143(1), 177-222, doi:https://doi.org/10.1007/s00211-019-01055-5.
- [9] Benzi, M., Faccio, C. (2024). "Solving linear systems of the form by preconditioned iterative methods", *SIAM Journal on Scientific Computing*, 46(2), S51-S70, doi:https://doi.org/10.1137/22M1505529.

- [10] Betts, J.T. (2020). "Practical methods for optimal control using nonlinear programming", Third Edition, SIAM Publication, doi:https://epubs.siam.org/doi/book/10.1137/1. 9781611976199.
- [11] Bhrawy, A.H. (2016). "A new spectral algorithm for time-space fractional partial differential equations with subdiffusion and superdiffusion", in *The Proceedings of the Romanian Academy Series A: Mathematics, Physics, Technical Sciences, Information Science*, 17(1), 39-47.
- [12] Chen, X., Zhao, T., Zhang, M.Q., Chen, Q. (2019). "Entropy and entransy in convective heat transfer optimization: A review and perspective", *International Journal of Heat and Mass Transfer*, 137, 1191-1220, doi:https://doi.org/10.1016/j.ijheatmasstransfer.2019.04.017.
- [13] Darehmiraki, M., Farahi, M.H., Effati, S. (2016). "A novel method to solve a class of distributed optimal control problems using Bezier curves", *Journal of Computational and Nonlinear Dynamics*, 11(6), 061008, doi:https://doi.org/10.1115/1.4033755.
- [14] Dohr, S., Kahle, C., Rogovs, S., Swierczynski, P. (2019). "A FEM for an optimal control problem subject to the fractional Laplace equation", *Calcolo*, 56(4), 37, doi:https://doi.org/10.1007/s10092-019-0334-3.
- [15] Ebrahimzadeh, A., Jajarmi, A., Baleanu, D. (2024). "Enhancing water pollution management through a comprehensive fractional modeling framework and optimal control techniques", *Journal of Nonlinear Mathematical Physics*, 31, 48, doi:https://doi.org/10.1007/s44198-024-00215-y.
- [16] Forsythe, G.E., Wasow, W.R. (1965). "Finite-Difference Methods for Partial Differential Equations", 3, New York, Wiley.
- [17] Garmanjani, G., Banei, S., Shanazari, K., Azari, Y. (2023). "An RBF-PUM finite difference scheme for forward–backward heat equation", *Computational and Applied Mathematics*, 42(5), 231, doi: https://doi.org/10.1007/s40314-023-02311-z.
- [18] Güttel, S., Pearson, J.W. (2022). "A spectral-in-time Newton-Krylov method for nonlinear PDE-constrained optimization", *IMA Journal of Numerical Analysis*, 42(2), 1478-1499, doi:https://doi.org/10.1093/imanum/drab011.
- [19] Han, H.G., Zhang, L., Qiao, J. (2023). "Dynamic optimal control for wastewater treatment process under multiple operating conditions", *IEEE Transactions on Automation Science and Engineering*, 20(3), 1907-1919, doi:10.1109/TASE.2022.3189048.
- [20] Kadum, R.M., Mahmoudi, M. (2023). "Solving optimal control problems governed by a fractional differential equation using the Lagrange matrix operator", *International Journal of Nonlinear Analysis and Applications*, 14(11), 299-308, doi:https://doi.org/10.22075/ijnaa. 2023.22167.3981.
- [21] Karumuri, S., Tripathy, R., Bilionis, I., Panchal, J. (2020). "Simulator-free solution of high-dimensional stochastic elliptic partial differential equations using deep neural networks", *Journal of Computational Physics*, 404(1), 109120, doi:https://doi.org/10.1016/j.jcp.2019. 109120.

- [22] Kırlı, E., Irk, D. (2023). "Efficient techniques for numerical solutions of Fisher's equation using B-spline finite element methods", *Computational and Applied Mathematics*, 42(4), 151, doi:https://doi.org/10.1007/s40314-023-02292-z.
- [23] Li, B., Wang, T., Xie, X. (2020). "Analysis of a time-stepping discontinuous Galerkin method for fractional diffusion-wave equations with nonsmooth data", *Journal of Scientific Computing*, 82(1), 4, doi:https://doi.org/10.1007/s10915-019-01118-7.
- [24] Li, L., Fu, Y., Yu, K., Alwakeel, A.M., Alharbi, L.A. (2022). "Optimal trajectory UAV path design based on Bezier curves with multi-hop cluster selection in wireless networks", *Wireless Networks*, 5021–5032, doi:https://doi.org/10.1007/s11276-022-03208-1.
- [25] Liu, T., Yu, J., Zheng, Y., Liu, C., Yang, Y., Qi, Y. (2022). "A nonlinear multigrid method for the parameter identification problem of partial differential equations with constraints", *Mathematics*, 10(16), 2938, doi:https://doi.org/10.3390/math10162938.
- [26] Mahmoudi, M., Shojaeizadeh, T., Darehmiraki, M. (2023). "Optimal control of time-fractional convection-diffusion-reaction problem employing compact integrated RBF method", *Mathematical Sciences*, 17, 1-14, doi:https://doi.org/10.1007/s40096-021-00434-0.
- [27] Martins, J.R.R.A. (2022). "Aerodynamic design optimization: Challenges and perspectives", *Computers & Fluids*, 239, 105391, doi:https://doi.org/10.1016/j.compfluid.2022.105391.
- [28] Mehandiratta, V., Mehra, M., Leugering, G. (2022). "Distributed optimal control problems driven by space-time fractional parabolic equations", *Control and Cybernetics*, 51(2), 191-226, doi: https://doi.org/10.2478/candc-2022-0014.
- [29] Mohsin Mohammed Ali, M., Mahmoudi, M., Darehmiraki, M. (2024). "Applying radial basis functions and partition of unity for solving heating equations optimal control issues", *Mathematical Modelling of Engineering Problems*, 11(12), 3402-3410, doi:https://doi.org/10.18280/mmep.111218.
- [30] Mophou, G.M. (2011). "Optimal control of fractional diffusion equation", Computers & Mathematics with Applications, 61(1), 68-78, doi:https://doi.org/10.1016/j.camwa.2010.10.030.
- [31] Odibat, Z., Baleanu, D. (2019). "A linearization-based approach of homotopy analysis method for non-linear time-fractional parabolic PDEs", *Mathematical Methods in the Applied Sciences*, 42(18), 7222-7232, doi:https://doi.org/10.1002/mma.5829.
- [32] Petrocchi, A. (2024). "Optimal input design for large-scale inverse problems using PDE-constrained optimization", *Dissertation in Mathematics and Statistics*, doi:http://nbn-resolving.de/urn:nbn:de:bsz:352-2-zfbkfhn8asg91.
- [33] Rizk-Allah, R.M., Hassanien, A.E., Marafie, A. (2024). "An improved equilibrium optimizer for numerical optimization: A case study on engineering design of the shell and tube heat exchanger", *Journal of Engineering Research*, 12(2), 240-255, doi:https://doi.org/10.1016/j.jer. 2023.08.019.
- [34] Salehi, Y., Schiesser, W.E. (2018). "Introduction to fractional partial differential equations", in *Numerical Integration of Space Fractional Partial Differential Equations: Vol 1 Introduction to Algorithms and Computer Coding in R*, pp. 1-33. Cham: Springer International Publishing.

- [35] Servadei, R., Valdinoci, E. (2014). "Weak and viscosity solutions of the fractional Laplace equation", *Publicacions Matemàtiques*, 58(1): 133-154.
- [36] Shah, F.A., Shah, K., Abdeljawad, T. (2025). "Numerical solution of two-dimensional time-fractional telegraph equation using Chebyshev spectral collocation method", *Partial Differential Equations in Applied Mathematics*, 13, 101129, doi:https://doi.org/10.1016/j.padiff. 2025.101129.
- [37] Shi, Z., Gulgec, N.S., Berahas, A.S., Pakzad, S.N., Takáč, M. (2020). "Finite difference neural networks: Fast prediction of partial differential equations", in *19th IEEE International Conference on Machine Learning and Applications, Miami, FL, USA*, 130-135, doi:10.1109/ICMLA51294. 2020.00029.
- [38] Sinigaglia, C., Manzoni, A., Braghin, F. (2022). "Density control of large-scale particle swarm through PDE-constrained optimization", *IEEE Transactions on Robotics*, 38(6), 3530-3549, doi: http://dx.doi.org/10.1109/TR0.2022.3175404.
- [39] Stanovov, V., Akhmedova, S., Semenkin, E. (2022). "NL-SHADE-LBC algorithm with linear parameter adaptation bias change for CEC 2022 numerical optimization", in *IEEE Congress on Evolutionary Computation*, Padua, Italy, 01-08, doi:10.1109/CEC55065.2022.9870295.
- [40] Stynes, M., O'Riordan, E., Gracia, J.L. (2017). "Error analysis of a finite difference method on graded meshes for a time-fractional diffusion equation", *SIAM Journal on Numerical Analysis*, 55(2), 1057-1079, doi:https://doi.org/10.1137/16M1082329.
- [41] Szabo, B., Babuska, I. (2021). "Finite element analysis: Method, verification and validation", *John Wiley & Sons Inc.*, doi:10.1002/9781119426479.
- [42] Tarigan, A.J.M., Mardiningsih, M., Suwilo, S. (2022). "The search for alternative algorithms of the iteration method on a system of linear equations", Sinkron: *Jurnal dan Penelitian Teknik Informatika*, 6(4), 2124-2424, doi:http://dx.doi.org/10.33395/sinkron.v7i4.11817.
- [43] Tushar, J., Kumar, A., Kumar, S. (2022). "Variational and virtual discretizations of optimal control problems governed by diffusion problems", *Applied Mathematics & Optimization*, 85(2), doi: https://doi.org/10.1007/s00245-022-09872-1.
- [44] Vabishchevich, P.N. (2020). "Approximation of a fractional power of an elliptic operator", *Numerical Linear Algebra with Applications*, 27(3), e2287, doi:https://doi.org/10.1002/nla.2287.
- [45] Yang, X., Li, S., Yuan, F., Dong, D., Huang, C., Wang, Z. (2023). "Optimizing multi-grid computation and parallelization on multi-cores", in *Proceedings of the 37th International Conference on Supercomputing*, 227-239, doi:https://doi.org/10.1145/3577193.3593726.
- [46] Ye, X., Xu, C. (2013). "A spectral method for optimal control problems governed by the time fractional diffusion equation with control constraints", in *Spectral and High Order Methods for Partial Differential Equations ICOSAHOM 2012: Selected papers from the ICOSAHOM conference, June 25-29, 2012, Gammarth, Tunisia,* 403-414. Cham: Springer International Publishing, doi:https://doi.org/10.1007/978-3-319-01601-6\_33.

- [47] Yuan, F., Yang, X., Li.S., Dong, D., Huang, C., Wang, Z. (2024). "Optimizing multi-grid preconditioned conjugate gradient method on multi-cores", *IEEE Transactions on Parallel and Distributed Systems*, 35(5), 768-779, doi:http://dx.doi.org/10.1109/TPDS.2024.3372473.
- [48] Zaky, M.A., Hendy, A.S., Macías-Díaz, J.E. (2020). "Semi-implicit Galerkin–Legendre spectral schemes for nonlinear time-space fractional diffusion–reaction equations with smooth and nonsmooth solutions", *Journal of Scientific Computing*, 82, 1-27, doi:https://doi.org/10.1007/s10915-019-01117-8.